Universiteit Utrecht

Opleiding Natuur- en Sterrenkunde

Electric-field-driven ionic transport on the nanoscale

Bachelor Thesis

R. van Asselt

Supervisors:

Prof. Dr. R.H.H.G. van Roij
Institute for Theoretical Physics

Dr. J. de Graaf
Institute for Theoretical Physics

MSc B. L. Werkhoven
Institute for Theoretical Physics

June 13, 2018

Abstract

In this thesis, we study the behaviour of a fluid containing both positive and negative charged ions, when this electrolyte is forced by an external electric field through a conical nanopore with a negative charged wall, by solving the Poisson-Nernst-Planck-Stokes (PNPS) equations numerically. We find that an external potential difference over this nanopore causes ionic transport which creates an electric current. We find the ion densities, total electric current. velocity and total potential as a function of the potential difference over the nanopore by varying this quantity for two different length scales of the geometry. We consider length scales such that in one of the geometries the Debye layers, caused by the charged pore wall, do not overlap in the pore. In the other geometry, we choose length scales such that these layers overlap in the pore. We find that the asymmetry in the geometry causes asymmetries with respect to the potential difference and that the length scale of the geometry has a huge impact on these, quantitative, asymmetries. Furthermore, we surprisingly find that peaks in the difference between the density of the positively and negatively charged ions do not shift into the pore if we increase the half-angle α.

Contents

1 Introduction

Transport of ions on the nanoscale is a physical phenomenon which has been an intense topic of research for over 20 years now. One of these researches is a recently released article from Laetitia Jubin, Anthony Poggioli, Alessandro Siria and Lydrric Bocquet called "*Dramatic pressure-sensitive ion conduction in conical nanopores*"[1]. In this article, the researchers claim that they found "a counterintuitive and highly nonlinear coupling between electric and pressure driven transport in a conical nanopore"[1](p. 1). The wall of this conical nanopore is negatively charged. Besides that, the research group measured the current as a function of a potential difference over this conical nanopore for a constant pressure. In the experiment, the group uses a nanopore with a length of about 3 mm, a maximum radius of 250 μm and a minimum radius of 165 $\pm$ 15 nm, from which follows that the so-called half angle, α, of the cone is about 5°[1] (p. 1). By varying the pressure-, ΔP, and potential difference, ΔV, between the inlet and outlet of the nanopore, Jubin et al. were able to find the electric current I as a function of these differences.[1]

The aim of this thesis is to consider a similar case as the experiment of Jubin et al. by determining aspects of the electrolyte flow numerically. We use a numerical model in *COMSOL Multiphysics 5.2*, which is described in Section 3 and which is based on the Poisson, Nernst, Planck, Stokes-equations, as derived in Section 2. In their experiment, Jubin et al. used a potassium chloride solution with a concentration of 1 mM at room temperature. Therefore, the Debye length is about 10 nm, as derived in Section 3.3. The Debye length gives a length scale for the width of the screening layer of the charged surface of the pore. Since the minimal width of the nanopore in the experiment is an order of magnitude bigger than the Debye length, there will be no overlap between the Debye screening layers in the nanopore, which means that there will be a region in the pore where the ions are not influenced by the charged pore wall. We deepen the experiment by varying the half angle α, but, in contrast to the experiment, we do not include pressure differences. To do that we have to develop a model with which we determine concentrations and the fluxes of these ions, which generate currents. Because the physics takes place at a length scale of the same order of magnitude as the Debye length, we choose the length scales of our model not to be much larger than these Debye length, otherwise, the numerical calculation time would be very large. Therefore, we choose our length scales such that the Debye screening layer would not overlap, since that is also the case in the experiment of Jubin, Poggioli, Siria and Bocquet, in our pore and that length of the pore is only two orders of magnitude larger than the Debye length. In addition to that, we create a model with length scales such that the Debye layers overlap in the pore.

Besides varying the potential difference, we thus also vary α, to see what happens with the current and ion densities when we change the shape of the conical pore. We vary α by keeping the length of the pore and the minimal radius constant and by varying the maximal radius. By varying both α and ΔV, we are able to give the current as a function of α and ΔV. Besides that, our model gives us the fluid velocity, total potential and density profiles in our system.

[1] In general they found I(ΔV) for fixed P and I(ΔP) for fixed V

The research gives an answer to the question. "What is the behaviour of an electrolyte forced by a potential gradient through a negatively charged conical nanopore?" In order to answer this question, we answer the following questions

- What are the density profiles of the different types of ions?
- What is the fluid velocity and the potential in the pore?
- What is the current through the pore?

To be able to solve these questions, we first derive the PNPS equations.

2 Derivation of the PNPS equations

2.1 Continuity equation

The first equation of the PNPS equations is the continuity equation. This equation follows from conservation of an extensive quantity. This quantity, with a density ρ, only changes by in or outflow, i.e. flux, $\mathbf{J}$. In integral form, the change of an extensive quantity q thus is given by [2]

$$\frac{dq}{dt} + \int_A \mathbf{J} \cdot \mathbf{n} dA = \delta \tag{2.1}$$

$$\frac{d}{dt} \int_V \rho dV + \int_V \nabla \cdot \mathbf{J} dV = \delta \tag{2.2}$$

$$\int_V \left(\frac{\partial \rho}{\partial t} + \nabla \cdot \mathbf{J} \right) dV = \delta, \tag{2.3}$$

where q is the extensive quantity, $\mathbf{n}$ the outward normal vector, δ the change of q, V the volume of the volume element and A its area . If q is conserved, $\delta = 0$, so

$$\frac{\partial \rho}{\partial t} + \nabla \cdot \mathbf{J} = 0. \tag{2.4}$$

In the case that there are several species, labelled by indices i, which keep their identity, i.e. no chemical reactions take place, the number of particles of each species is conserved, so the continuity equation, as stated in (2.4), holds for all different species i and is given by

$$\frac{\partial \rho_i(\mathbf{r}, t)}{\partial t} + \nabla \cdot \mathbf{J}_i(\mathbf{r}, t) = 0, \tag{2.5}$$

where $\mathbf{J}_i(\mathbf{r},\mathrm{t})$ is the particle flux of species i and $\rho_i(\mathbf{r},\mathrm{t})$ its particle density.

2.2 Nernst-Planck equation

For the flux of a particle of species i, there are several contributions. First of all the diffusive flux, which follows from Fick's first law as $\mathbf{J}^{dif} = -D\nabla\rho$, where D is the diffusivity (which has the unit $\mathrm{m^2 s^{-1}}$).[3] If we again consider different particles, labelled by index i, Fick's first law reads

$$\mathbf{J}_i^{dif} = -D_i \nabla \rho_i. \tag{2.6}$$

Secondly, there could be a contribution from conduction. This flux follows from external forces and friction. One could determine the conductive flux by Newton's second law. Since the Reynolds number is small, which will be proven in Section 3.3, the viscosity dominates the flow. Hence, the acceleration of a particle is zero, so that a particle only has a velocity when there is a force acting on it. The friction force on a particle is given by Stokes law[4], $\mathbf{F}_{fric} = -\gamma \mathbf{v}$, with γ the friction coefficient. For spherical particles, which we consider to be

the case for our species, γ is given by $6\pi\eta a_i$, with a_i the hydrodynamic radius of species and η the dynamic viscosity i[4]. Newton's second law thus is given by

$$0 = \mathbf{F}_{ext} + \mathbf{F}_{fric} \tag{2.7}$$
$$= \mathbf{F}_{est} - \gamma\mathbf{v} \tag{2.8}$$
$$\mathbf{v} = \frac{\mathbf{F}_{ext}}{\gamma}. \tag{2.9}$$

Therefore, the velocity of a particle in an electric field, for which $\mathbf{F}_{ext} = z_i e\mathbf{E}$, with z_i the valency of species i and e the unit charge, in a low Reynolds number flow is

$$\mathbf{v}_E = \frac{z_i e\mathbf{E}}{6\pi\eta a_i} \tag{2.10}$$
$$= \frac{D_i}{k_B T} z_i e\mathbf{E}, \tag{2.11}$$

where D_i is, by the fluctuation-dissipation relation, determined to be $D_i = \gamma_i k_B T$,[5] such that the conductive flux, density times velocity, from an electrical field is given by

$$\mathbf{J}_i^{cond,E} = \rho_i \mathbf{v}_E \tag{2.12}$$
$$= \rho_i \frac{D_i}{k_B T} z_i e\mathbf{E}. \tag{2.13}$$

Another external force that could give particles velocity, is a forces that follows from a potential U_i. This force thus is equal to $\mathbf{F}$ = -∇U, so that the velocity caused by this potential is given by.

$$\mathbf{v}_U = -\frac{D_i}{k_B T}\nabla U_i, \tag{2.14}$$

such that the conductive flux from this potential is

$$\mathbf{J}_i^{cond,U} = -\rho_i \frac{D_i}{k_B T}\nabla U_i. \tag{2.15}$$

Finally there could be a flux caused by fluid flow. For different kinds of particles, this flux will again be density times velocity, but now this velocity is equal to the velocity of the fluid flow. So this convective flux will be

$$\mathbf{J}_i^{conv} = \rho_i \mathbf{u}, \tag{2.16}$$

where $\mathbf{u}$($\mathbf{r}$,t) is the velocity of the fluid flow.

Combining these four fluxes and introducing the electric potential V with $\mathbf{E}$ = -∇V, which we prove in Section 2.3, will give the total flux of species i as

$$\mathbf{J}_i = -D_i\left(\nabla\rho_i + z_i\rho_i\beta e\nabla V - \rho_i(\mathbf{r},t)\beta\nabla U_i\right) + \rho_i\mathbf{u}). \tag{2.17}$$

This equation is called the Nernst-Planck equation.

2.3 Poisson Equation

The Poisson equation could be derived from one of Maxwell's equations. Gauss' law (in a linear material) reads $\nabla \cdot \mathbf{E} = \frac{\rho_f}{\epsilon_0 \epsilon}$,[6] where ρ_f is the free charge density, ϵ the dimensionless relative permittivity and ϵ_0 the permittivity in vacuum. Now we assume that there will be no time dependence of the magnetic field, since we consider steady states, then Faraday's law reads $\nabla \times \mathbf{E} = 0$,[6] so $\mathbf{E}$ follows from a potential, or $\mathbf{E} = -\nabla \mathrm{V}$. We substitute this in Gauss's law and find that

$$\nabla \cdot (\nabla V) = \nabla^2 V = -\frac{\rho}{\epsilon_0 \epsilon} \tag{2.18}$$

$$\epsilon_0 \epsilon \nabla^2 V = -\rho = -\left(Q_{\text{ext}} + e \sum_i z_i \rho_i \right) = -Q_{\text{ext}} - e \sum_i z_i \rho_i, \tag{2.19}$$

where ρ is the total free charge and ρ_i is free charge density of species i. Furthermore, Q_{ext} is the external charge. We used that the total free charge density follows from an external charge and the charge density of the different species.

2.4 (Navier)-Stokes equation

As shown in Section 2.1, the continuity equation follows from conservation of mass (or conservation of particles). Since momentum is also conserved, this conservation law will give another continuity equation. Consider a fluid element with mass density ρ, volume V and area A, which, since we are looking for a steady state solution, do not depend on time. Newton's second law then gives[2]

$$\frac{d}{dt} \int_V \rho \mathbf{u} dV = \int_V \rho \mathbf{g} dV + \int_A \mathbf{f} dA \tag{2.20}$$

$$\int_V \frac{\partial}{\partial t} (\rho \mathbf{u}) dV + \int_A \rho \mathbf{u} (\mathbf{u} \cdot n) dA = \int_V \rho \mathbf{g} dV + \int_A \mathbf{f} dA, \tag{2.21}$$

where Reynolds Transport Theorem is used to rewrite (2.20) as (2.21).[2]. In these equations $\mathbf{g}$ is the body force per unit mass, $\mathbf{f}$ the surface force per area and $\mathbf{u}$ the velocity. Now use tensor notation and the fact that $\mathrm{f_j}(\mathbf{n},\mathbf{r},\mathrm{t}) = \mathrm{n_i T}_{ij}$, with T_{ij} the stress tensor which is equal to $\mathrm{T}_{ij} = -p\delta_{ij} + \tau_{ij}$, with p the pressure and τ_{ij} the stress from fluid-dynamics.[2] From this, (2.21) becomes (by using Gauss' theorem to write the surface integrals as volume integrals)

$$\int_V \left(\frac{\partial}{\partial t} (\rho u_j) + \frac{\partial}{\partial x_i} (\rho u_i u_j) - \rho g_j - \frac{\partial}{\partial x_i} T_{ij} \right) dV = 0, \tag{2.22}$$

where g_j is the j^{th}-component of the total body force per unit mass. Now use that, for Newtonian and incompressible fluids, the stress tensor could be written as[2]

$$T_{ij} = -p\delta_{ij} + 2\eta S_{ij}, \tag{2.23}$$

with η the dynamic viscosity and S_{ij} the strain rate tensor, which is defined as

$$S_{ij} = \frac{1}{2} \left(\frac{\partial u_i}{\partial x_j} + \frac{\partial u_j}{\partial x_i} \right). \tag{2.24}$$

Since (2.22) must hold for arbitrary volumes, the integrand from (2.22) should be zero. Furthermore, we could write out the first to terms of the integrand as

$$\frac{\partial}{\partial t}(\rho u_j) + \frac{\partial}{\partial x_i}(\rho u_i u_j) = \rho\frac{\partial u_j}{\partial t} + u_j\left[\frac{\partial \rho}{\partial t} + \frac{\partial}{\partial x_i}(\rho u_i)\right] + \rho u_i \frac{\partial u_j}{\partial x_i} = \rho\frac{du_j}{dt}, \tag{2.25}$$

an use that the term between the square brackets is zero by (2.4). Now we substitute (2.23) and (2.25) into the integrand from (2.22) to find that

$$\rho\frac{du_j}{dt} - \rho g_j - \frac{\partial}{\partial x_i}\left[-p\delta_{ij} + \eta\left(\frac{\partial u_i}{\partial x_j} + \frac{\partial u_j}{\partial x_i}\right)\right] = 0 \tag{2.26}$$

$$\rho\frac{du_j}{dt} - \rho g_j + \frac{\partial p}{\partial x_j} - \eta\left(\frac{\partial}{\partial x_j}\frac{\partial u_i}{\partial x_i} + \frac{\partial^2 u_j}{\partial x_i^2}\right) = 0 \tag{2.27}$$

$$\rho\frac{du_j}{dt} - \rho g_j + \frac{\partial p}{\partial x_j} - \eta\left(\frac{\partial}{\partial x_j}\frac{\partial u_i}{\partial x_i} + \frac{\partial^2 u_j}{\partial x_i^2}\right) = 0. \tag{2.28}$$

Another property of an incompressible fluid is that the velocity is divergence free, or in tensor notation $\frac{\partial u_i}{\partial x_i} = 0$. (2.28) then reduces to

$$\rho\frac{du_j}{dt} - g_j + \frac{\partial p}{\partial x_j} - \eta\left(\frac{\partial^2 u_j}{\partial x_i^2}\right) = 0, \tag{2.29}$$

or

$$\rho\frac{d\mathbf{u}}{dt} = -\nabla p + \rho\mathbf{g} + \eta\nabla^2\mathbf{u}, \tag{2.30}$$

which is known as the Navier Stokes equation for incompressible flow. When a flow is very viscous, the Reynolds number is very small. This tells that the advective terms are much smaller than the viscous terms, so that this non linear equation could be written as the linear equation

$$\rho\frac{\partial\mathbf{u}}{\partial t} = -\nabla p + \rho\mathbf{g} + \eta\nabla^2\mathbf{u}, \tag{2.31}$$

which is the Navier Stokes equation without the advection term, also known as the Stokes equation.

Finally, one could use that an example for a body force per volume follows from an electostatic potential. Then, $\rho\mathbf{g}$ = -e$\nabla\psi\sum_i z_i\rho_i$. Substituting (2.19) and assuming that there are no external charges then gives

$$\rho\frac{\partial\mathbf{u}}{\partial t} = -\nabla p + \eta\nabla^2\mathbf{u} + \epsilon_0\epsilon(\nabla^2 V)\nabla V. \tag{2.32}$$

We consider a two dimensional axisymmetrical systems with velocity vector $\mathbf{u} = (u, v, w)^T$, such that v, the angular velocity, is zero, which contains one species of positively and one species of negatively charged ions. Therefore we find six differential equations for six variables (ρ_+, ρ_-, u, w, V and p), which we state in Section 3.2. To solve these equations we use the method that we describe next.

3 Numerical model

The numerical program that we use to solve the PNPS equations, as derived in Section 2, is *COMSOL Multiphysics*. In this program, which in general can be used to numerically solve differential equations on a grid, several physical problems can be solved by using predefined modules. In order to do that, we first build our geometry and grid. Besides, we implement the physics into the model and define for which parameters we want to solve the physics. But first of all, we note that we consider a steady state solution, to make the numerical work a little bit easier.

3.1 Geometry and mesh

First of all, we build our geometry, which consists of a conical channel with length L, minimal radius R_0 and maximal radius R_1 and which is shown in Fig. 1, in *COMSOL*. By defining these length scales, we find that the so-called half angle, α of the conical channel is calculated by $\tan(\alpha) = (R_1 - R_0)/L$, which follows quite easily from Fig. 1. Above and beyond the channel, we build two cylindrical reservoirs, with a radius which is twice the pore length. We use these reservoirs to properly define boundary conditions, since, for example, the ground potential should be defined far away from the system. The purple axis in Fig. 1 is the symmetry axis of the system, around which the whole system is rotationally symmetric, such that the reservoirs are cylinders and the channel is conical. The connections between the channel wall and the reservoirs are circular corners, with a radius of $R_0/4$. In order to solve the PNPS equations numerically, we use three predefined modules in *COMSOL*; Transport of diluted species (TDS), Electrostatics (ES) and Creeping Flow (CF). The modules contain all physical aspects that we need to solve the PNPS equations. Besides that, we define a grid, or as it is called in *COMSOL*, a mesh. This mesh is very important for the model in order to solve the equations defined in the modules. Since an extremely fine mesh means that the time that is needed for the calculations will be quite large, we define this mesh in a smart way. We define the mesh in the reservoir quite coarse, since the physics does not takes place in the reservoirs. We use the physical settings from *COMSOL* to form triangles with a size that *COMSOL* bases on physical settings. In these "physical settings" we

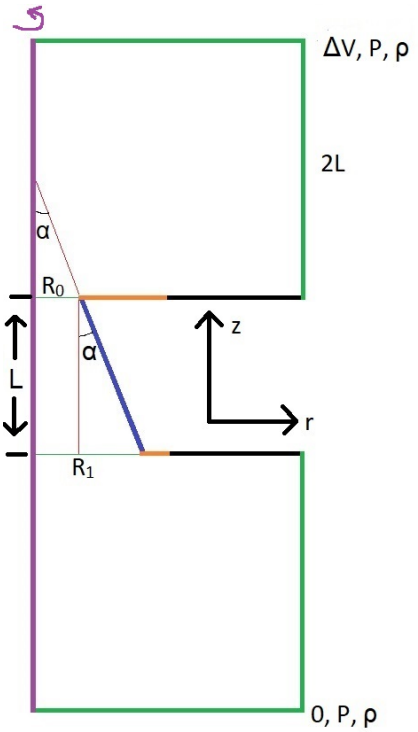

Figure 1: *2D representation of the axisymmetric geometry. The purple axis is the symmetry axis around which the whole system is rotation symmetric, such that the reservoirs are cylinders and the channel in conical. The length of channel is L, the minimum radius is R_0 and the maximum radius is R_1, the reservoirs have radius that is twice the channel length.*

define the mesh to be "normal". Since the actual physics happens in the conical channel, the mesh in the channel has to be very fine. We use again triangles to mesh the system, but now the sizes of the triangles are way smaller than the sizes in the reservoirs. Since the length scales at which the physics takes place are one order of magnitude smaller than the minimal radius of the channel, which we derive in Section 3.3, we choose the maximal size of the triangles to be $R_0/20$ in the case that we deal with non overlapping Debye layers and $R_0/10$ in the case that we considered overlapping Debye layers. To now solve the PNPS equations, we define these equations in the way we want to solve them in the predefined modules. In principle, these modules already contain the standard form of the PNPS equations, but we modify them that we solve exactly the equations we want to solve.

3.2 Modifying physical modules

In the first module, TDS, we define that the system contains KCl, so we have one species of positively charged ions, with a valency of 1, and one species of negatively charged ions, with a valency of -1. The diffusion coefficient of both ions is about 10^{-9} m^2s^{-1}. Besides that, we define that the ions move by the fluid flow generated in CF and the electric potential defined in ES. Furthermore, we have to define the boundary conditions for the denisty of the potassium, ρ_+, and chloride, ρ_-, ions. At the green walls, shown in Fig. 1, we define the densities to have a fixed value of 1 mM. By using this boundary condition, we numerically define the reservoirs to be infinitely large. We also define a no-flux boundary condition for the black, orange and blue walls.

The ES module has to be modified too. First of all, we define charge conservation in the whole system. Also, the fluid which contains the potassium and chloride ions is water, which has, at room temperature, a relative permeability of $\epsilon = 78.2$ [7]. At the black walls of the geometry shown in Fig. 1, we define zero charge, at the blue wall we define a constant charge density of -eσ, with $\sigma = 0.05$ nm^{-2} the electron density at the surface, and at the orange walls we define the density to linearly decrease from -eσ at the connection point with the channel wall to 0 halfway the reservoir. At the green walls we define the boundary conditions for the potential. In the lower reservoir, the potential is grounded and in the upper reservoir, the potential is set to a variable value ΔV. Furthermore, since a density difference between potassium and chloride gives a volume charge density which is equal to $(\rho_+ - \rho_-)N_a e$, with N_a the Avogadro number, we define this volume charge density in the whole system.

Finally, we define boundary conditions and external force terms to the CF module. First of all, we neglect the advective term in the Navier-Stokes equation, as stated in (2.30), since we consider a flow on nanoscale so the viscosity dominates the flow, which gives that the Reynolds number is very small, as we derive in Section 3.3. Furthermore, we define that we have to deal with an incompressible flow. Besides, we define that water is the fluid that flows, with a density of about 1000 kg m^{-3} and a dynamic viscosity of about 10^{-3} Pa s. At the black, orange and blue walls we define a no slip boundary condition and at the green walls we define the boundary conditions for the pressure, which is equal to the reference pressure (1 atm) in both the upper and lower reservoir. Finally, we have to add a volume force to the Stokes equation, as stated in (2.31). The external force is generated the electric

field, such that we replace $\rho\mathbf{g}$ in (2.31) by -$N_a e(\rho_+ - \rho_-)\nabla V$, which is derived in Appendix A.

By modifying the physical modules, we let *COMSOL* solve the following equations

$$\mathbf{J}_i = -D_i\left(\nabla\rho_i + z_i\rho_i\beta e\nabla V\right) + \rho_i\mathbf{u}, \tag{3.1}$$
$$\nabla\cdot\mathbf{J}_i = 0, \tag{3.2}$$
$$\epsilon_0\epsilon\nabla^2 V = -e(\rho_+ - \rho_-)i, \tag{3.3}$$
$$0 = -\nabla p + \eta\nabla^2\mathbf{u} - eN_a(\rho_+ - \rho_-)\nabla V, \tag{3.4}$$
$$\nabla\cdot\mathbf{u} = 0, \tag{3.5}$$

where (3.1) follows from the Nernst-Planck equation (2.17) without a non electric potential, (3.2) from the continuity equation (2.4) in steady state, (3.3) from the Poisson equation (2.19) without an external charge distribution and where the ionic charge is the free charge, (3.4) from the Stokes-equation (2.31) in steady state and (3.5) from the continuity equation (2.4) since the density of water is constant and we consider a steady state.

Now that we defined our model and the physics that we add, we define our parameters and state what we do to obtain results.

3.3 Settings and execution

In order to be able to solve the PNPS equations numerically, we have to define the parameters for which we solve these equation. The chosen parameters are shown in Table 1, in which $\rho_{\pm,r}$ is the density in the reservoir for the positively and negatively charged ions. Since we define the surface charge of the channel to be -eσ, as stated in Section 3.2, the pore wall is negatively charged.

Table 1: *Chosen values and their unit for the different, but constant, parameters. Here, $\rho_{\pm,r}$ is the density of the positively or negatively charged particles in the reservoirs and σ is the electron density at the pore wall.*

Parameter	Value	Unit
$\rho_{+,r}$	1	mol m^{-3}
$\rho_{-,r}$	1	mol m^{-3}
σ	0.05	nm^{-2}

From these values, we could determine some important features of our model. First of all the Debye length, which is, in water, defined as[8]

$$\lambda_d = \left(\frac{\epsilon_w\epsilon_0 k_B T}{e^2\sum_i \rho_i z_i^2}\right)^{1/2} = \left(\frac{\epsilon_w\epsilon_0 k_B T}{e^2(\rho_+ + \rho_-)}\right)^{1/2}, \tag{3.6}$$

which gives that the Debye length for our system, which is at room temperature, by substituting the parameters from Table 1 and the known physical constants, is about 10 nm. In the remaining, we consider two cases. First of all, we define a geometry where the Debye

layers do not overlap. Since the Debye length gives the length scale at which the potential caused by a charged surface decreases by a factor of e, there will be a region in the pore where the potential from the charged wall is negligible. If we chose the minimal width one order of magnitude larger than the Debye length, it is possible for the negatively charged ions to relatively easily move through the pore, despite the fact that the wall of the channel is negatively charged too, since in the middle of the pore, they do not feel the potential by the charged wall.[8] For the second case, we consider a minimal width of the channel which is of the same order of magnitude as the Debye length. Then, it would be way more difficult for the negatively charged particles to move through the pore, because the effects of the charged pore wall are present throughout the pore. For the two different cases, the values for R_0 and L are stated in Table 2

Table 2: *Chosen values and their unit for the length scales of our system. Here, R_9 is the minimal width of the pore and L its length.*

Parameter	Value (no overlap)	Value (overlap)	Unit
R_0	100	15	nm
L	1000	100	nm

Since we are interested in the current and density profiles as a function of the potential difference over the two reservoir, we vary ΔV from -400 to 400 mV in steps of 100 mV. We are also interested in the influence of the geometry of the nanopore on the behaviour of the ions, so we varied the angle α from 0 to 10 degrees in steps of 2 degrees. We varied α by keeping the minimal width, R_0, and length ,L, of the pore constant and by varying the maximal width R_1. We let *COMSOL* solve the PNPS equation, as stated in Section 3.2 for all combinations of the different parameters.

COMSOL solves the six differential equations as stated in Section 3.2, for the seven variables in these equations, which we stated in Section 2.[2] With these values, we determine some other physical aspects like the density (difference) profiles and the total electric current through the channel. To determine the density difference profile ($\rho_+ - \rho_-$), we average the density difference over r and look what these profiles are as a function of z. To do this, we use the linear projection operator (linproj) in *COMSOL*. In Appendix B we specify how to properly define the linear projection operator in *COMSOL*. Shortly said, the operator integrates the argument over r, such that $\text{linproj}(x) = \int dr x$,[3] so the mean density, as a function of z is given by

$$\langle \rho_\pm \rangle(z) = \frac{1}{\pi (R(z))^2} \int_0^{R(z)} dr 2\pi r \rho_\pm(r,z) = \frac{\int_0^{R(z)} dr 2\pi r \rho_\pm(r,z)}{\int_0^{R(z)} dr 2\pi r}, \tag{3.7}$$

$$= \frac{\text{linproj}(2\pi r \rho_\pm)}{\text{linproj}(2\pi r)}. \tag{3.8}$$

[2]There are eight equations given in Section 3.2, but *COMSOL* solves these combining (3.1) and (3.2)

[3]Note that COMSOL does not include the Jacobian and the integration over the angle (around which is the whole system is symmetric)

Since *COMSOL* also computes the total flux of both particles, we calculate the total current through the pore. We use the internal molecular flux as defined in *COMSOL* to determine the total current, I, through the channel by

$$I(z) = \int_0^{R(z)} dr 2\pi r(J_+ - J_-)N_a e = N_a e \cdot \text{linproj}(2\pi r(J_{+,z} - J_{-.z})), \tag{3.9}$$

with $J_{+,z}$ and $J_{-,z}$ the flux in z-direction of the potassium and chloride ions respectively.

Besides these variations in z direction, we also want to show what the behaviour of the fluid with ions is in the r direction. Therefore, we make representations of the velocity, potential and density difference as a function of r at $z = 0$. To show more details of the velocity and potential, we use the in *COMSOL* generated 2D representations for the velocity and potential. In case of the velocity profiles, it is useful to determine the Reynolds number, which is a motionlessness number that gives the ratio between the inertial forces and the viscous term in the Navier-Stokes equation (2.30). The Reynolds number is found by making this equation dimensionless and it is defined as $\text{Re} = \rho u L/\eta$. Since we consider the nanoscale, we expect the velocity to be in the order of cm/s maximally. In both our geometries, the chosen L is in the order of μm, so by substituting $\rho = 1000$ kg/m^3 and $\eta = 10^{-3}$ Pa s, we find that the Reynolds number is about 10^{-2}, so the inertial forces are much smaller than the viscous terms, so (2.30) reduces to the Stokes equation (2.31)

By considering the density profiles, velocity, potential and current, we think we could give a good description of the behaviour of the fluid in the pore.

4 Results

In the Results section, we distinguish between the two different geometries. We also comment on the results for the individual pore-geometries and we will compare these observations in Section 5. We will first start by describing and interpreting the results for length scales, $R_0 = 100$ nm and $L = 1000$ nm (such that we consider this geometry to be the large pore geometry), where there is no overlap of the Debye layers in the pore.

4.1 Large pore-geometry

As described in Section 3.3, we want to find the density, velocity and potential profiles. Besides we determine the electric current through the pore. We vary the potential difference ΔV from -400 to 400 mV in steps of 100 mV and α from 0 to 10 degrees in steps of 2 degrees, such that we get a set of six geometries for which we calculate the stated properties. In this section we will show the results for the pore with length scales such that the Debye layers do not overlap. We will first show the density profiles.

4.1.1 Density profiles

First of all, we need to give a definition for what we mean with "density profile". Because the system has a charged pore wall, we are interested in the difference between the density of the positively and negatively charged particles, so by "density profile" we mean $\rho_+(r,z) - \rho_-(r,z)$. For these density profiles, we find, for the case that $\alpha = 0°$, that the density profiles are symmetric in the $z = 0$ plane for $\Delta V = 0$. This is expected, since the geometry is symmetric for these parameters. The case that $\Delta V = 0$ is the state that the system is not forced by any external force, so this is called the equilibrium state. We show the density profiles with respect to the equilibrium state, because the shape of the profile does not change a lot by varying ΔV, but by subtracting the equilibrium state, we are able to show that the profiles change if we vary ΔV.

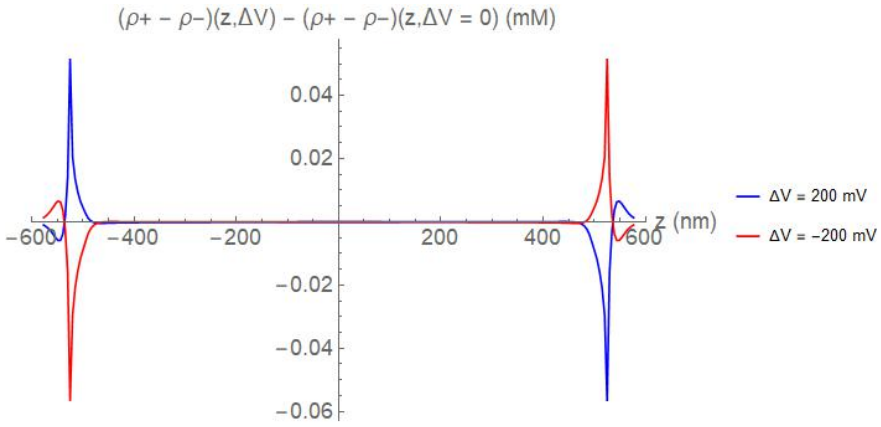

Figure 2: *Over r averaged density profile $(\rho_+ - \rho_-)$ with respect to equilibrium $(\Delta V = 0)$ for $\Delta V = \pm 200$ mV and $\alpha = 0$. We see that figure is antisymmetric with respect to the potential difference ΔV.*

In Fig 2, we show this density profile as a function of z, where we averaged over the radial coordinate r. In this figure, we show the over r averaged density difference, $\langle \rho_+ - \rho_- \rangle(z)$, for $\Delta V = \pm 200$ mV minus the density difference in equilibrium ($\Delta V = 0$) for $\alpha = 0$. We clearly see that the figure is antisymmetric with respect to the potential difference. If we change the sign of the potential difference, the location of the maximum and minimum changes location but keeps the same value for the averaged density difference. This is what is expected, since $\alpha = 0°$ means a cylindrical pore, such that the ions do not feel the charged pore wall more if they are forced to move into the pore from the one or other side. Also the location of the peaks shown in Fig. 2 makes sense since, for general α, we expect that the positively and negatively charged ions are forced to move in opposite directions by an external potential difference. For $\Delta V > 0$ we expect the negatively charged ions to move in positive z direction and the positively charged ions in negative z direction. For negative ΔV we expect them to move in the opposite direction. Therefore, we expect a density difference $(\rho_+ - \rho_-)$ averaged over r with respect to equilibrium ($\Delta V = 0$) between the upper and lower reservoir if we apply an external potential difference. For positive ΔV we expect this difference to be negative in the upper reservoir and positive in the lower reservoir and for negative ΔV we expect this the other way around, which we see in Fig. 2.

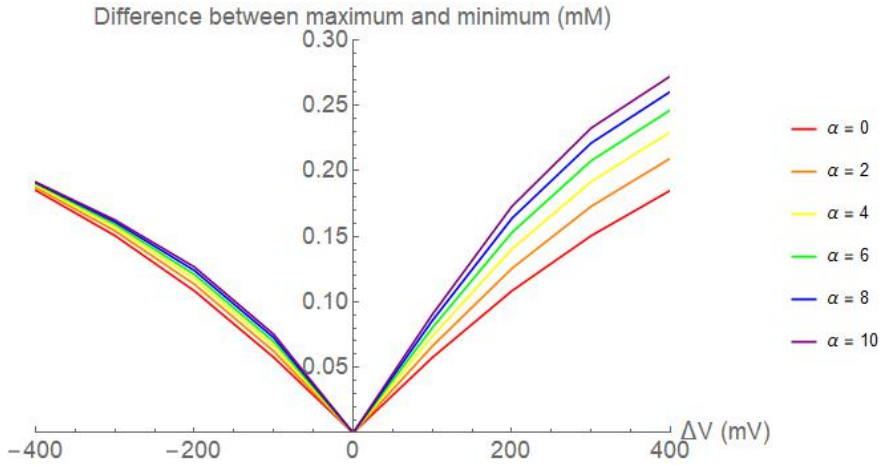

Figure 3: *Difference between the maximum and minimum of the density difference $(\rho_+ - \rho_-)$ with respect to equilibrium for all evaluated values of α. The asymmetry between positive and negative ΔV is discovered.*

However, we see that there is a difference between the maxima and minima in the density profile with respect to equilibrium. We show this difference in Fig, 3 for all values of α as a function of the potential difference. In Fig. 3 we see that the difference between the maximum and minimum of the density difference with respect to equilibrium increases by increasing $|\Delta V|$. This makes sense, since the magnitude of electric force, as stated in Section 2, goes linearly with $\mathbf{E}$ and thus, by $\mathbf{E} = -\nabla V$, increases with increasing $|\Delta V|$. Therefore the ions are forced to separate more, such that difference between the maxima and minima of the density profile increases with increasing $|\Delta V|$, which we see in Fig. 3. In this figure, we also see the symmetry with respect to the potential for the case that $\alpha = 0°$, i.e. we see that the difference between the maximum and minimum of the over r averaged density difference is the same for, for example, $\Delta V = \pm 200$ mV. For the case that $\alpha \neq 0°$, we see an asymmetry

with respect to ΔV. This asymmetry in the potential difference for $\alpha \neq 0$ follows from the fact that the pore in this case is conical and thus no longer symmetric in the $z = 0$ plane.

Because of the asymmetry in the geometry, the influence of the charged wall in the upper reservoir differs from the influence in the lower reservoir. Therefore, we do not expect symmetries with respect to ΔV any more, which we see in Fig. 3. We see that, for negative ΔV, the difference between the maximum and minimum of the density difference with respect to equilibrium is about the same for all evaluated values of α. This is because for this geometry the minimal radius of the conical pore is the same as the radius of the cylindrical one. Therefore, the influence of the charged pore wall at the connection with the upper reservoir is the same for all values of α and thus, the negatively charged ions, which are forced to move in negative z direction, flow into the pore in the same way for all values of α. Because of that, the charge in the pore is the same, since the positively charged ions are not blocked by the pore when they move in positive z direction. Therefore the difference between the maximum and minimum of the density difference with respect to equilibrium will be about the same for all values of α. In Fig. 3 we also see that the differences between the minimum and the maximum increases by increasing α for positive ΔV. A larger value of α means that the influence of the charged pore wall at the connection with the lower reservoir is smeller. Therefore, the force of the pore wall, which repels the negatively charged particles, is, averaged over the channel width, smaller for larger values of α. Therefore, there will be more negatively charged ions in the channel. At the connection with the upper reservoir, the physics is not changed by increasing α, since the radius of the pore is fixed at that point. But since there are more negatively charged ions in the pore for larger values of α, the force that attracts the positively charged ions in the pore, is larger for larger values of α. Because of this effect, the difference between the densities of the positively and negatively charged ions in the upper reservoir is larger, for larger values of α and therefore, the difference between the maximum and minimum of the density profile with respect to equilibrium in the steady state increases by increasing α, which we see in Fig. 3.

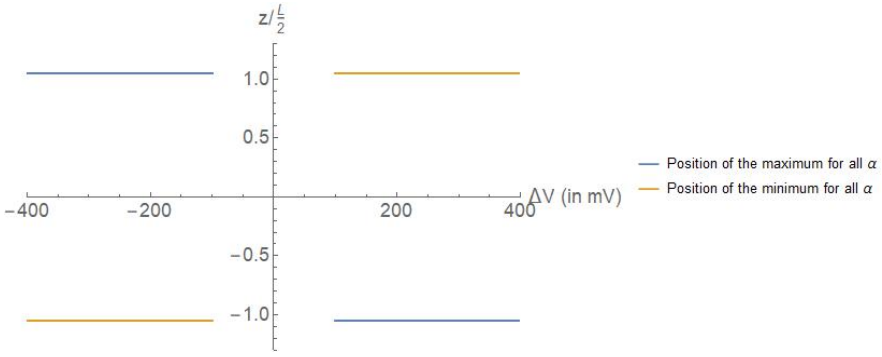

Figure 4: *Position of the minimum and maximum of the density difference ($\rho_+ - \rho_-$) with respect to equilibrium ($\Delta V = 0$) as a function of the density difference ΔV for all evaluated values of α. We see that the positions of the maximum and minimum do not change if we charge α.*

We also determine the position of the peaks, showed in Fig. 2 for the case that $\Delta V = \pm 200$ mV, for the different values of ΔV and α, which results in Fig. 4. In this figure, we see that the location of the peaks does not change for different values of α and ΔV (only for $\Delta V = 0$ we see that there are no peaks and thus no location of the peaks, since we look at the density difference with respect to equilibrium). We see that the position of the peaks is at $z = 525$ nm for all values of α., which is where the reservoirs start, since at $z = \pm 500$ nm there is a circular corner with a radius of 25 nm. This is a quite surprising results, because for larger values of α the influence of the charged pore wall becomes less at the connection of the pore with the lower reservoir. Therefore, we expected the position of the minimum and maximum to shift inside the pore for larger values of α, but Fig. 4 shows that this does not happen. Since we consider a large pore such that the Debye layers do not overlap in the pore, the influence of the charged pore wall is not present near the main axis of the pore. Therefore, increasing α does not influence the system as much as it will do in the case of the small pore, because in that case it will change the influence of the charged pore wall on the main axis of the pore. This is one of the reasons why we consider this geometry too.

For the large pore, we also determine the density difference as a function of r in the middle of the channel, which results in Fig.5.

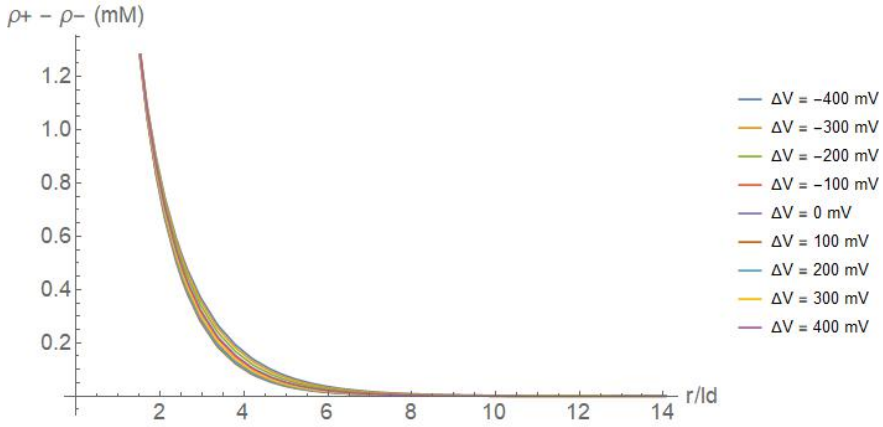

Figure 5: *Density difference between the the positively and negatively charged ions as a function of the distance from the wall of the pore for different values of* ΔV *evaluated at* $z = 0$ *for the large pore with* $\alpha = 4°$.

In this figure, we see that the influence of the negatively charged pore vanishes at the main axis of the pore, since the minimal radius of the pore is about one order of magnitude larger than the Debye length. We conclude this since the density difference $(\rho_+ - \rho_-)|_{z=0}$ vanishes after about four Debye lengths away from the charged pore wall. We see that the density difference is affected a little bit by the potential difference, but that these differences are minor. We see that the structure of the density difference profile is determined by the charged pore wall, since the external potential difference does not change the shape of the profile.

With these findings, we complete the description of the density profile in the nanopore. We will now give the results concerning the total electric current and discuss these results.

4.1.2 Electric current

We determine the total electric current in z direction as a function of the potential difference and show it in Fig. 6a for different values of α. In this figure the asymmetry for positive and negative ΔV, that we see in the density difference, is not discernible. To show this asymmetry, we calculate the difference between the current for $\Delta V = -400$ mV and the absolute value of the current for $\Delta V = 400$ mV and we make this dimensionless by dividing by the sum of both to show the relative magnitude of this asymmetry. The results are shown, as a function of α, in Fig. 6b.

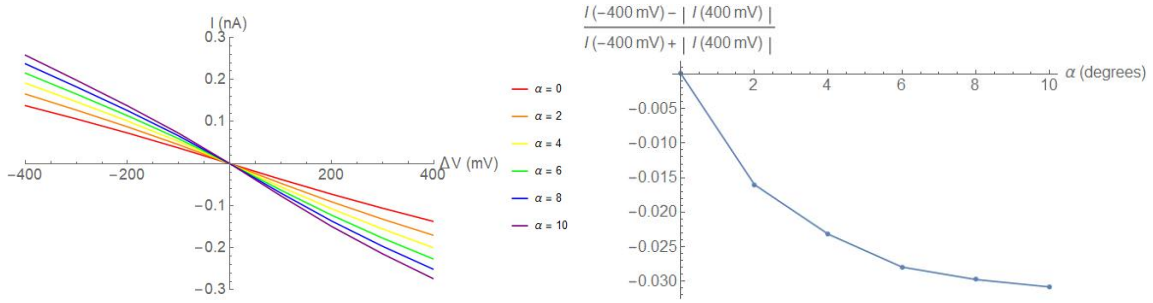

(a) (b)

Figure 6: *a) The total current, as calculated by* (3.9)*, as a function of the potential difference* ΔV *for different values of* α *for the large pore-geometry. b) The difference between the current for* $\Delta V = -400$ *mV and the absolute value of the current for* $\Delta V = 400$ *mV divided by the sum of both as a function of* α *for the large pore geometry.*

We see that the current, for constant ΔV increases by increasing α. This makes sense, since the density difference gradient in z direction for the density difference becomes larger if α increases, as shown in Fig. 3. Since the peaks in the density difference remain at the same position, but the difference increases by increasing α, the density difference gradient will increase by increasing α, such that the total current will also increase. At equilibrium, we notice that the current is zero, which makes sense, since ions do not move in equilibrium. We also see a small asymmetry in the current for positive and negative ΔV for $\alpha \neq 0°$, which is shown in Fig. 6b. We besides see that the absolute value of the current for positive ΔV is larger than it is for negative ΔV. Note that we show the difference between the currents for $\Delta V = \pm 400$ mV, because by increasing the potential difference, we expect the difference in the currents to be larger, such that we could see any relations between α and the asymmetry with respect to ΔV in the current faster. We see that the difference increases by increasing α, which makes sense, since the asymmetry in the pore is more present at larger values of α. Interestingly, it seems like the asymmetry in the current will reach an asymptote if we increase α further. This makes sense, since the force by the charged pore wall is, for all evaluated values of α, small in on the main axis of the pore, since the potential is constant for $r \gtrsim 4\lambda_d$. The force at the connection with the lower reservoir becomes smaller by increasing α, but for some value of α the force is already so small that the ions are not affected any more in the middle of the channel, such that the total electric current does not become more asymmetric. We have to note that this asymmetry is relatively small compared to the electric current itself, as shown in Fig. 6b. This is expected, since there are, for all values of α regions

in the pore where there is no influence of the charged pore wall, because the minimal radius of the pore is one order of magnitude larger than the Debye length.

4.1.3 Velocity and potential profile

As mentioned in Section 3.3, we also generate results regarding the velocity and the potential profile. We use the by *COMSOL* generated 2D representations of the velocity and potential to show the profile of both quantities in the pore. The results for the velocity are shown in Figure 7 for $\Delta V = -300$ mV and $\Delta V = 300$ mV for $\alpha = 8°$. We also give the velocity in z direction for $\alpha = 4°$ as a function of r at $z = 0$ for all evaluated potential differences. The results are shown in Fig. 8a. In Fig. 8a, we see that, for all potentials, the boundary

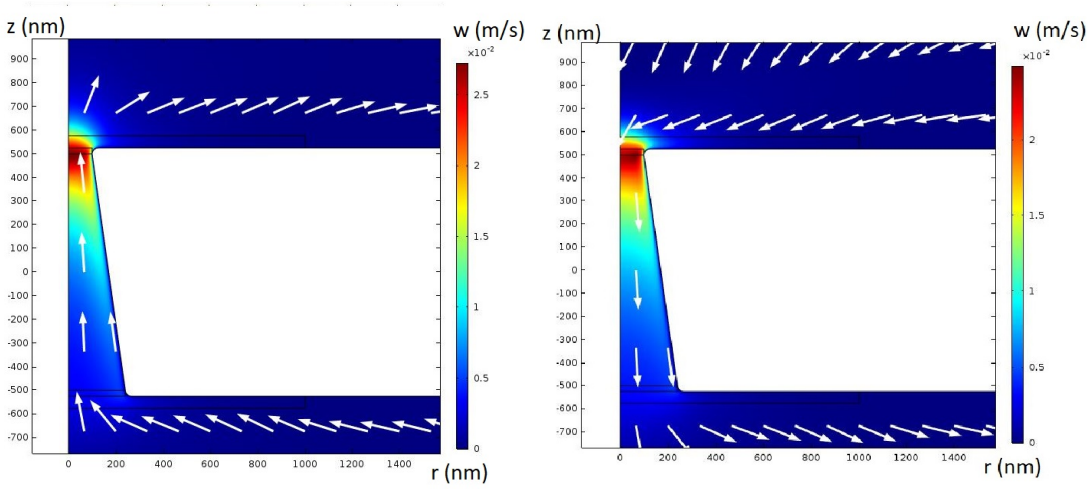

(a) (b)

Figure 7: *Velocity in the pore for $\alpha = 8°$ for the large pore. The white arrows show the normalised velocity field. a) shows the velocity for $\Delta V = -300$ mV and b) shows it for $\Delta V = 300$ mV.*

condition, that the velocity at the charged wall is zero, is satisfied. Furthermore, we see that the velocity profiles for the different potentials look equal in shape. This shape is a strong growth in the velocity in the Debye layer (which has a width of about 4 Debye lengths) and that the velocity outside the Debye layer decays a little bit towards a constant, which depends on the potential difference. We notice that in equilibrium, $\Delta V = 0$, there is no velocity as expected. Furthermore, we see that the (average) velocity is larger if we increase $|\Delta V|$, which makes sense since then the potential gradient (in z direction) will increase and, by (3.4), the Laplacian of the velocity will become large and therefore the velocity itself becomes larger. In Fig. 7 we see for the velocity at $\alpha = 4°$ that the direction of the velocity changes by changing the sign of ΔV, which we can explain by considering (3.4). Since we do not apply a pressure gradient, we expect this term does not dominate the equation, such that the velocity is fully determined by the potential gradient, so if the gradient changes direction, the velocity will too. Furthermore, we see that the velocity is largest at the minimal width of the pore, this is because of the divergence free character of the stationary flow, so this result is also explainable by the physics of the system.

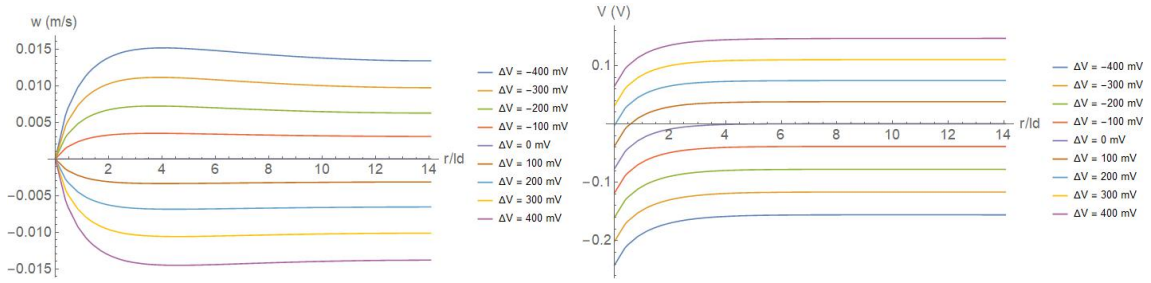

(a) (b)

Figure 8: *a) The velocity of the flow in z direction for the large-pore geometry with $\alpha = 4°$ as a function of r, the distance from the pore wall evaluated at $z = 0$ for all evaluated potential differences ΔV. b) The total potential as a function of r at $z = 0$ for the large pore-geometry with $\alpha = 4°$ for all evaluated ΔV.*

The 2D representation of the potential is shown in Fig. 9 for $\Delta V = \pm 300$ mV for $\alpha = 8°$ and the potential as a function of r at $z =$ is shown in Fig. 8b. In this figure we see, for ΔV = 0, the characteristics of the Debye layer. As discussed in Section 3.3, we see that the potential goes to zero within a couple of Debye lengths. Furthermore, an external potential gradient only shifts the potential by a constant. This is, because in absence of a charged pore wall, the potential will increase (or decrease) linearly over the pore. Therefore, in the middle of the pore, the potential is about half of the value of ΔV. We see this shift in the total potential, because the width between the lines for different potential are about 50 mV apart, which is half of the step sizes between the imposed external potential difference. Fig. 8b is shown for $\alpha = 4$ degrees, but we see that qualitatively nothing changes if we change α. This could be expected, since α does not influence the Debye layer and potential difference and does therefore not influence the total potential. If we now consider the 2D representation of the potential, for $\alpha = 8°$ and $\Delta V = \pm 300$ mV, as shown in Fig. 9, we see that the direction of the electric field changes if we change the sign of ΔV, which makes sense, since the external potential is the only potential difference in z direction. If we look closely at the pore wall, we see that the potential is negative, which follows from the negatively charged pore wall. Also, for $\Delta V = 300$ mV, we see that this negative potential almost disappears at the minimal width of the channel, so that the negatived charged ions are not affected by the negative charged wall there, which we stated earlier in this section. We also see that the potential decreases linearly as a function of z throughout the pore.

With the results and discussion for the velocity and total potential of the system, we have given a description of the system for the large pore. In the next section, we will give a description for the small pore, in which the Debye layers overlap to see what the influence is of the length scale of the geometry on the physical results.

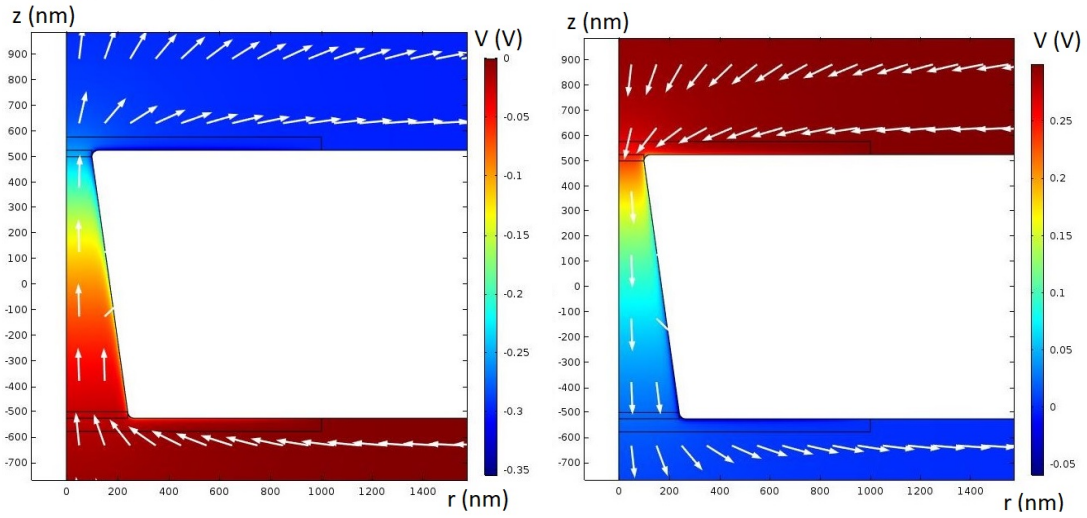

(a) (b)

Figure 9: *Potential in the pore for $\alpha = 8°$ for the large pore. The white arrows show the normalised electric field. a) shows the potential for $\Delta V = -300$ mV and b) shows it for $\Delta V = 300$ mV.*

4.2 Small pore-geometry

For the length scale of the pore at which the Debye layers overlap, $R_0 = 15$ nm and $L = 100$ nm (such that we consider this to be the small pore), we again varied ΔV from -400 to 400 mV in steps of 100 mV and α from 0 to 10 degrees in steps of 2 degrees. To be able to compare this results with the results for a pore where the Debye layers do not overlap, we again determine the density profile, total electric current, the velocity and potential profile.

4.2.1 Density profiles

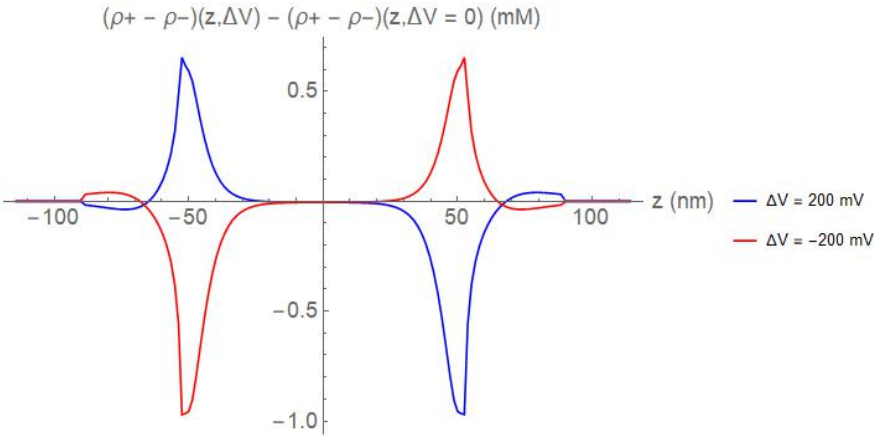

Figure 10: *Over r averaged density profile $(\rho_+ - \rho_-)$ with respect to equilibrium $(\Delta V = 0)$ for $\Delta V = \pm 200$ for the small-pore geometry with $\alpha = 0$. We see that the figure is antisymmetric with respect to the potential difference ΔV*

We determine the over r averaged density profile as a function of ΔV and z, again with respect to equilibrium ($\Delta V = 0$). The results for $\Delta V = \pm 200$ mV and $\alpha = 0°$ are shown in Fig. 10. We again notice the symmetry with respect to ΔV in this figure, which we expected by the symmetry in the geometry. We do again see an asymmetry with respect to z, which is because of the charged channel wall. In this figure, we see that the difference between the densities of the ions (with respect to equilibrium) is again zero for $\alpha = 0°$ in the pore. However, we see that the peaks are about one order of magnitude larger than they are for the large pore and that the peaks are relatively wide and not sharply peaked. In order to see the asymmetries with respect to ΔV for $\alpha \neq 0$, we again determined the difference between the peaks of averaged over r density profile with respect to equilibrium and show this in Fig. 11. In this figure, we again see that the case that $\alpha = 0$ corresponds to a symmetry with respect to ΔV in the difference between the two peaks with respect to ΔV, which is expected by the symmetry in the geometry.

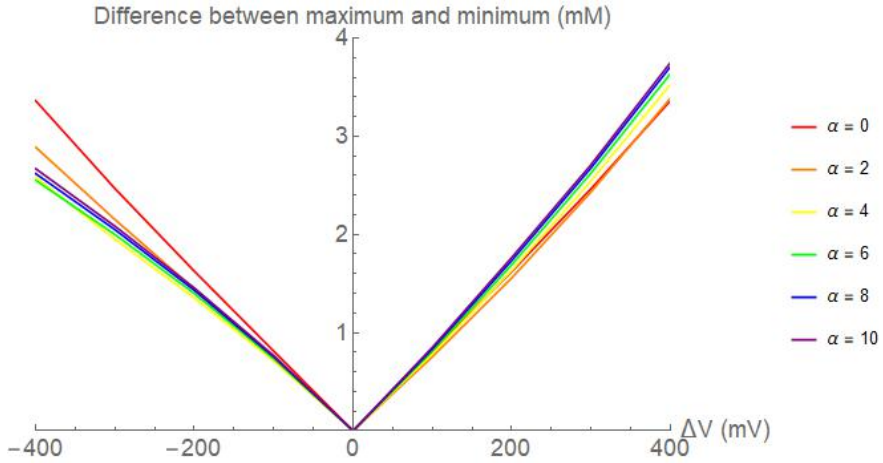

Figure 11: *Difference between the maximum and minimum of the density difference ($\rho_+ - \rho_-$) with respect to equilibrium ($\Delta V = 0$) for the small pore for all evaluated values of α. The asymmetry between positive and negative ΔV is discovered.*

For $\alpha \neq 0°$ we see that there is some asymmetry with respect to ΔV in the difference between the maxima and minima of the density profile with respect to equilibrium. Interestingly, we now see that the difference does not change much for positive ΔV, but it does change for negative values of ΔV. For all values of α that we evaluated, we see a difference from the case that $\alpha = 0°$, but we also see that the difference looks quite the same for α is 4, 6, 8 and 10 degrees. This could be explained by the overlapping Debye layers in this pore-geometry. Since the force of the charge wall is in this case not small on the main axis of the pore, it is very hard for the negatively charged ions to travel through the minimal width of the pore, because the overlap of the Debye layers at that z coordinate is maximal. Also the positively charged ions are affected by this Debye layer, because they are attracted by the wall. Therefore, for positive potential differences, it is very hard for the negatively charged particles to move in positive z direction, because the Debye layers will overlap more and more by increasing z for $\alpha \neq 0°$. The overlap is maximal at the minimum width of the pore, at which the overlap is the same as it is for the case that $\alpha = 0°$. Therefore, the density profiles will not change a lot for positive ΔV, because of the block that is formed by the overlapping

Debye layers at the connection with the upper reservoir. This block will be cancelled by the external potential more and more if this potential increases. The difference between the maximum and minimum in the density difference profiles thus becomes larger with increasing ΔV.

The drop in the difference in the peaks for negative ΔV for increasing α is a bit harder to explain. For negative ΔV, the negatively charged particles are forced to move in negative z direction, but since the Debye layers overlap at the connection between the upper reservoir and the pore, there movement is countered. On the other hand, the positively charged ions are forced to move in the positive z-direction and are attracted by the pore wall. Because of the fact that the external potential is more negative than the potential by the charged wall, the positively charged ions will move in positive z direction. If α increases, the effect of the charged wall on the positively charged ions at the connection with the lower reservoir is less than it is for the case that $\alpha = 0°$. Therefore, the peak in the lower reservoir will decrease, so the difference between the two peaks will decrease as well. We think that this could be the explanation for the behaviour of the fluid which is shown in Fig. 11, but further studies will probably give better insight.

Besides, we look at the positions of this maximum and minimum. Surprisingly, as shown in Tables 3 and 4, which are stated in Appendix C, the positions of the maximum and minimum do not shift much if we increase α, but they keep their positions around z = $\pm$ 50 nm, the beginning of the reservoir. We make a table of this results, because the shifts are very small and therefore not good discernible in a figure. We see that the positions of the maxima and minima do shift, but that these shifts are very small. We see that these largest (but still small) shifts take place at the largest potential difference and $\alpha = 10°$. This suggests that there might be a relation between the location of the peaks and the half angle of the conical nanopore. However, we have to note that the shifts of the peaks are minor, since we determined averaged over r density profile on a grid, such that the shifts of the peaks is only one or two grid points. We thus think that these shifts are rather a numerical error than an actual shift. To make sure our thoughts, we suggest further research, i.e. making the potential difference and α larger, on the location of the peaks, but for now we consider that the peaks do not shift by increasing α. This is, in our opinion, the most interesting result of this thesis, since we expected that the position of the maxima and minima in the lower reservoir would shift into the pore if we increase α.

Finally, we determine the density difference with respect to r at $z = 0$ for $\alpha = 4°$ and show this in Fig. 12. In this figure, we see that, as for the large pore, the potential does not influence the shape of the density profile at $z = 0$. We see, in the case of the small pore, the density difference does not go to zero on the main axis on the pore, but it drop to a constant. This is because of the overlapping Debye layers, such that the influence of the charged pore wall is present throughout the pore.

With these findings, we have been able to give an insight in the density profiles of the ions in teh small pore-geometry.

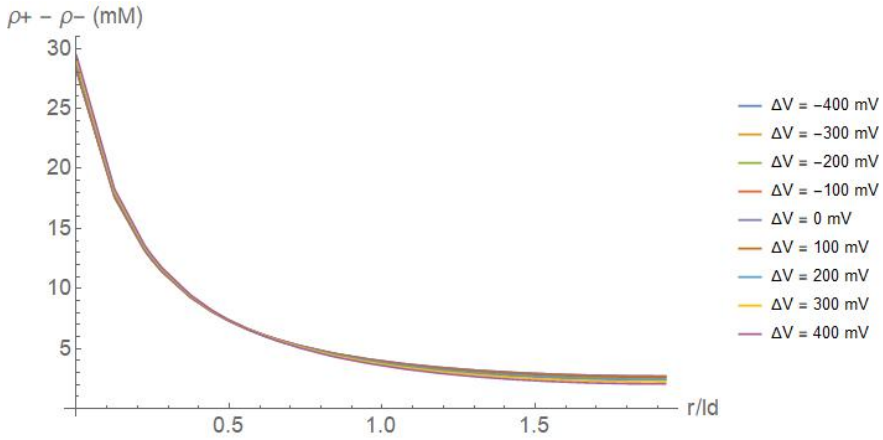

Figure 12: *Density difference between the the positively and negatively charged ions as a function of the distance from the wall of the pore for different values of* ΔV *for the small pore with* $\alpha = 4°$.

4.2.2 Electric current

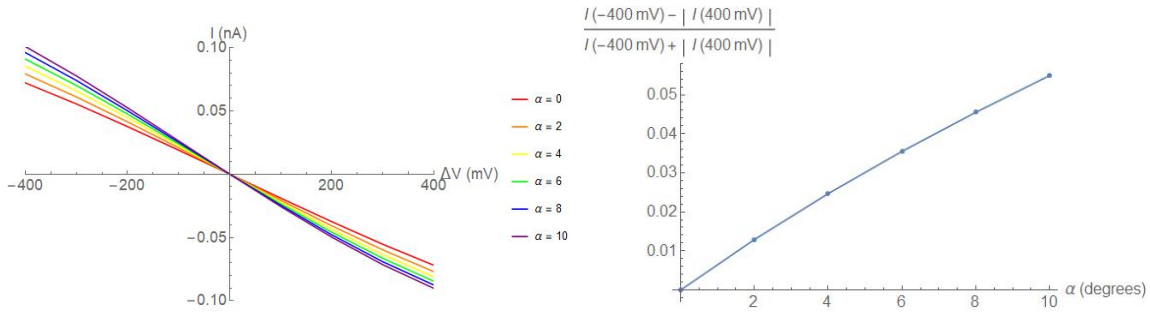

(a) (b)

Figure 13: *a) The total current, as calculated by* (3.9)*, as a function of the potential difference* ΔV *for different values of* α *for the small pore-geometry. b) The difference between the current for* $\Delta V = -400$ *mV and the absolute value of the current for* $\Delta V = 400$ *mV divided by the sum of both as a function of* α *for the small pore-geometry.*

We also determine the total current through the pore. The current as a function of the potential difference is shown in Fig. 13a for different values of α. We see that the total current is three times smaller than it is for the geometry with the large pore. However, the shape of the current profile for the small pore is quite the same as it is for the large one, since we again see that this current is positive for negative values of ΔV, zero in equilibrium and negative for positive values of ΔV. We also see that the difference between the curves for different values of α is smaller than is was for the large pore. However, if we determine the difference between the current for ΔV = -400 mV and the absolute value of the current for ΔV = 400 mV and divide this by the sum of both to make the expression dimensionless, as shown in Fig. 13b, we find an asymmetry with respect to the potential difference. This asymmetry becomes larger by increasing α, which follows from the fact that the system is

more and more asymmetric for increasing α. Interesting is the fact that the current for $\Delta V = -400$ mV is now larger than the absolute value of the current for $\Delta V = 400$ mV, which we will discuss in Section 5.

4.2.3 Velocity and potential profile

Finally, for the small pore we also determine the velocity and potential. We again use the by *COMSOL* generated 2D representations for the velocity, which we show in Fig. 14 for $\alpha = 8°$ and $\Delta V = \pm 300$ mV.

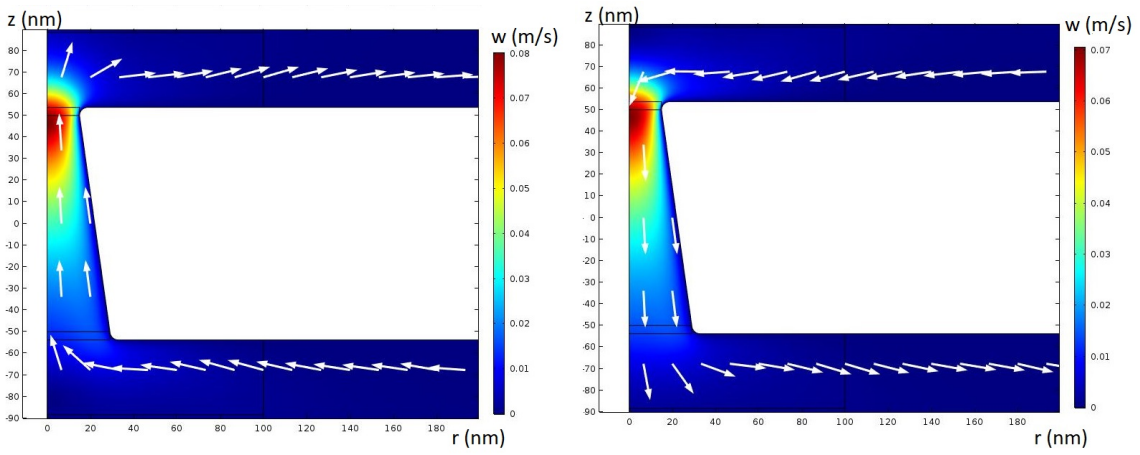

(a) (b)

Figure 14: *Velocity in the pore for $\alpha = 8°$ for the small pore. The white arrows show the normalised velocity field. a) shows the velocity for $\Delta V = -300$ mV and b) shows it for $\Delta V = 300$ mV.*

If we look at the velocity profiles, we see that the z component of the velocity at $z = 0$, increases towards an asymptote if we move away from the charged wall for all potential differences, which we show in Fig. 8a. This means that the velocity increases within the Debye layer, which is the same as in the case that we considered the large pore. If we look at the 2D representations of the velocity, that are shown in Fig. 14, we see that again the velocity has a maximum at the minimal width of the pore and changes direction if ΔV changes sign. We thus observe the same properties for the velocity as we did earlier for the large pore.

The potential, however, does change if we change the pore-geometry. In Fig. 15b we see that the potential for $\Delta V = 0$ is negative throughout the width of the pore. This is because of the fact that the Debye layer is throughout the pore, so the potential will always be negative in equilibrium. We see that the spacing between the different potential differences is not constant. This is because of the fact that a negative potential difference strengthens the Debye layer and a positive potential difference cancels it. This difference that the Debye layer overlap occurs is also discernible in the 2D representation of the potential at $\alpha = 8°$, which is shown in Fig. 16. We see that the cancellation of the Debye layer is the same, but we also see that the charged pore wall has influence near the main axis of the pore. The latter is also clear from the density difference, which is shown in Fig. 12.

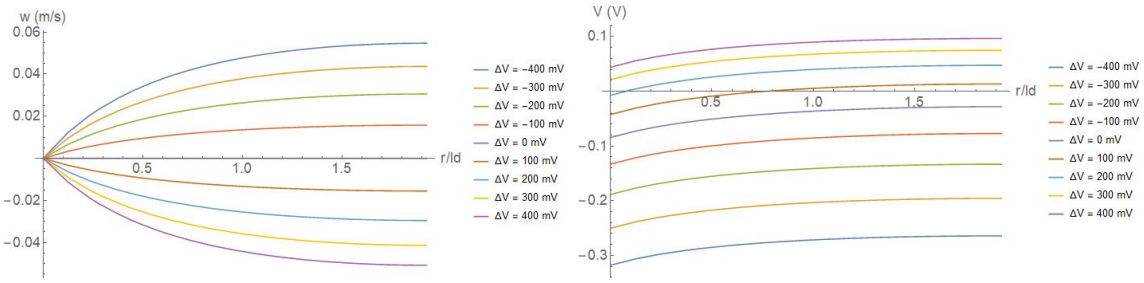

(a) (b)

Figure 15: *a) The velocity of the flow in z direction for the small pore-geometry with $\alpha = 4°$ as a function of the distance from the pore wall, r, evaluated at $z = 0$. b) The total potential a a function of r at $z = 0$ for the small pore-geometry with $\alpha = 4°$.*

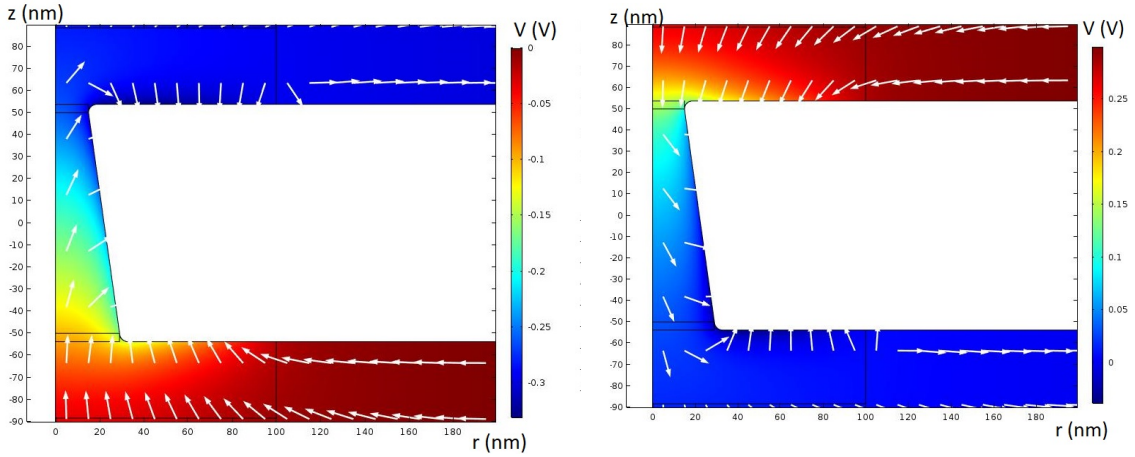

(a) (b)

Figure 16: *Potential in the pore for $\alpha = 8°$ for the small pore. The white arrows show the normalised electric field. a) shows the potential for $\Delta V = -300\ mV$ and b) shows it for $\Delta V = 300\ mV$.*

With these figures we have completed our results and discussing of the individual pore-geometries. In the next section we will discuss the differences and similarities between both geometries..

5 Discussion and outlook

First of all, we see that the density profiles change a lot by changing the geometry. We see that the density difference in pore becomes larger in the small pore-geometry than it is in the large one. This makes sense, because in the Debye layer, the negatively charged particles are repelled, and the positively charged ions are attracted, such that the difference between the density of the two kinds is the greatest in the Debye layer. In both pore-geometries, the density distribution with respect to equilibrium gives two peaks which are located just outside the pore. For both pore-geometries, these peaks do not shift in position if we change α, which is, especially in the case that we considered the small pore, not expected. Because increasing α means that the negatively charged ions go easier into or out of the pore in the lower reservoir than they do in the upper reservoir. For the large pore, the charged pore wall already does not influence the electrolyte in the middle of the pore, such that the influence of α is considered smaller.
The asymmetry in the difference between the maximum and minimum of the density difference profile is different for the two pore-geometries. For the large pore, the difference of the peaks does not change significantly as a function of α for negative ΔV, where the difference of the peaks in the small pore does not change for positive ΔV. This is a quite surprising result, since the physics of both settings are the same. Therefore we can conclude that the length scale of the system changes the physics, so that it matters a lot for flows on nanoscale what the exact length scale is.

For the total electric current, we also find a difference between the two pore-geometries. In the large pore the absolute value of the current is larger for positive ΔV, but for the small pore, the current is larger for negative ΔV. We think that there might be some analogy between this and the change in the asymmetry of the density profile.

In case of the velocity, potential and density profiles as a function of r, we see that qualitatively the same things happen for both pore-geometries. We see that the velocity increases in the Debye layer and then goes to a constant value in both geometries. The potential is affected by both the external potential and the potential of the charge wall. Therefore, the potential in the small pore is different from the potential in the large one, because the influence of the charged pore wall changes if we consider another pore-geometry. The density profiles as a function of r are as expected, since they decay within the Debye layer to zero in the large pore and to a constant value in the small pore, since in the latter, the Debye layer from the other side of the pore influences the potential and thus the density profile in the middle of the pore as well.

There are also some quantitative differences between the two pore-geometries. First of all, the total electric current is about three times bigger in the large pore, but because in that case the radius of the pore is one order of magnitude larger than the radius of the small pore, the current per area would be about two orders of magnitude smaller in the large pore than it is in the small pore. This is expected, since the selectivity of a pore with overlapping Debye layers is bigger than it is for a pore with non overlapping Debye layers. Besides, the velocity of the fluid is one order of magnitude bigger in the small pore, but that could be expected,

since the radius of this pore is an order of magnitude smaller than it is in the case for the large pore, so, in order to keep the divergence free character of the velocity, the velocity is larger in the small pore.

With these observations, we think that we can give a good view of the behaviour of an electrolyte forced by an external electric field on the nanoscale.

6 Conclusion

By applying an electric potential difference over a nanopore with a charged pore wall, we are able to find the behaviour of an electrolyte that is forced to move through this nanopore. By varying the potential difference and the shape of the cone (from cylindrical to conical by changing the so-called half angle α) for two different length scales of our geometry, we find a density profile (the difference between the densities of the positively and negatively charged ions) which contains two peaks if we compare this profile to equilibrium ($\Delta V = 0$). These two peaks are located just above and beyond the pore in both pore-geometries. We find that these peaks do not move inside the channel if we increase α, which we expected to happen in case of the pore-geometry with length scales such that the Debye layers overlap in the pore, as explained in Section 5. We find the asymmetries in the difference between this peaks as a function of the potential difference over the system for $\alpha \neq 0°$. When $\alpha = 0°$, the pore-geometries are symmetric in the $z = 0$ plane such that aspects like the density profile and total electric current are symmetric with respect to ΔV. In case that $\alpha \neq 0$, we find asymmetries with respect to ΔV in both the peak difference and the total electric current, which is shown in Section 4. The asymmetries change if we change the length scales of the pore. If we choose the length scales such that the Debye lengths overlap in the pore (this case we call small pore), we find that the peak difference is different from the case that $\alpha = 0°$ for positive ΔV. However, the peak difference for the pore-geometry for which the Debye layers do not overlap in the pore (which we call the large pore) is different from the case that $\alpha = 0°$ for negative ΔV.

In case of the total electric current, the asymmetry also changes when we change the pore-geometry. For the large pore, the current for positive ΔV is larger than it was for negative ΔV, but in the small pore we find that this is the other way around. Because of the fact that the change of geometry changes the behaviour of the current en density profiles qualitatively, we first of all conclude that the asymmetric aspects of the fluid on the nanoscale is heavily depending on the fact if the Debye layers overlap in the nanopore or not.

Besides, we find that the velocity of the fluid and the potential of the system qualitatively are as expected, as explained in Section 5. We see that in both pore-geometries, the velocity in z direction, at fixed z, increases in the Debye layer and then goes to a constant. We find that the potential is negative at the charged wall of the pore and that this potential goes to zero within a couple of Debye lengths if we do not apply an external potential difference ΔV in case of the large pore. Besides, for the small pore we find that the potential caused by the charged pore wall goes to a non-zero constant in middle of the pore, which is because of the shape of the pore. We see that an external potential difference changes the total potential as expected qualitatively.

With the in Section 4 given density profiles, fluid velocity, electric potential and current we manage to give an insight in the aspects of a flowing electrolyte on the nanoscale. We find asymmetries in the current and density profiles if we consider a conical nanopore, which do depend on the length scale of the pore. Furthermore, we see that the peaks of the density profile with respect to equilibrium are located just outside the pore for all values of α. This

is a surprising result, especially for the small pore geometry, because increasing α means less influence of the charged pore wall. We recommend further research on this behaviour, by increasing the half-angle α, such that the influence of the charged pore at the connection with the lower reservoir wall will decrease more and more.

References

[1] L. Jubin, A. Poggioli, A. Siria, and L. Bocquet, Dramatic pressure-sensitive ion conduction in conical nanopores **115** (2018), URL http://www.pnas.org/content/pnas/115/16/4063.full.pdf.

[2] P. K. Kundu, I. M. Cohen, and D. R. Dowling, *Fluid Mechanics* (Academic Press, 2016), 6th ed., ISBN 978-0-12-405935-1.

[3] H. Mehrer, *Diffusion in solids* (Springer Berlin Heidelberg, 2007), ISBN 978-3-540-71486-6.

[4] M. Fowler, *Stokes' law*, URL https://phys.libretexts.org/Core/Fluids/1.7%3A_Stokes%E2%80%99_Law.

[5] R. Kubo, The fluctuation-dissipation theorem p. 257 (1966), URL http://stacks.iop.org/0034-4885/29/i=1/a=306.

[6] D. J. Griffiths, *Introduction to Electrodynamics* (Pearson Education Limited, 2014), 4th ed., ISBN 978-1-292-02142-3.

[7] encyclopaedia Britannica, *Dielectric cosntant*, URL https://www.britannica.com/science/dielectric-constant.

[8] A. M. Smith, A. A. Lee, and S. Perkin, The Electrostatic Screening Length in Concentrated Electrolytes Increases with Concentration (2016), URL https://arxiv.org/ftp/arxiv/papers/1607/1607.03926.pdf.

[9] C. Ruhl, Analyze your Simulation Results with Projection Operators (2016), URL https://www.comsol.com/blogs/analyze-simulation-results-projection-operators/.

A Derivation volume force term in Creeping Flow module

The external force term in the CF module has two terms. The ∇V term follows from the Lorentz force law without an electric field: $\mathbf{F}$ = q$\mathbf{E}$, with q the charge and $\mathbf{E}$ the electric field. The force per volume therefore is $\mathbf{g}$ = -$\rho_q \nabla$V, where ρ_q is the charge density and where $\mathbf{E}$ = -∇V is substituted. The charge density is equal to the sum over the densities of particles times their charge, or $\rho_q = \sum_i z_i e \rho_i$. In our case, we consider one species of positively charged particles and one species of negatively charged particles, so $\rho_q = N_a e(\rho_+ - \rho_-)$, where the factor N_a is encountered because COMSOL gives us densities in mol m^{-3} and we need a density in m^{-3}.

B Linear Projection Operator

For the Linear Projection Operator in *COMSOL*, which in principal projects our 2D rotational symmetric system on a line. To properly do that, first select the domain at which the operator has to work. Then we define source en destination vertices in operator. Source vertex 1 is the starting point of integration, we define this on the symmetry axis at the beginning of the channel in the upper reservoir. Source vertex 2 is the end point of integration, so we define this vertex on the symmetry axis at the beginning of the channel in the lower reservoir. Source vertex 3 is the direction of integration, so we define this vertex at the channel wall, at the beginning of the channel in the upper reservoir. We have to define two destination vertices too, these are the same as Source vertex 1 and 2. To learn more about the Linear Projection Operator for a pipe flow, one could read an article by Clemens Ruhl.[9]

C Tables

Table 3: *Position of the maxima in the density difference ($\rho_+ - \rho_-$) with respect to equilibrium for the small pore, such that the Debye layers overlap in the pore, for all evaluated values of potential difference ΔV and half-angle α. Note that a value -1 corresponds to the connection with the lower reservoir and 1 corresponds to the connection with the upper reservoir.*

ΔV (in mV)	z coordinate (divided by $L/2$) for different α					
	0	2	4	6	8	10
-400	1.05	1.05	1.05	1.05	1.05	1.05
-300	1.05	1.05	1.05	1.05	1.05	1.05
-200	1.05	1.05	1.05	1.05	1.05	1.05
-100	1.05	1.05	1.05	1.05	1.05	1.05
100	-1.05	-1.05	-1.075	-1.075	-1.075	-1.075
200	-1.05	-1.075	-1.075	-1.075	-1.075	-1.075
300	-1.05	-1.075	-1.075	-1.075	-1.075	-1.075
400	-1.05	-1.075	-1.075	-1.075	-1.075	-1.075

Table 4: *Position of the minima in the density difference ($\rho_+ - \rho_-$) with respect to equilibrium for the small pore, such that the Debye layers overlap in the pore, for all evaluated values of potential difference ΔV and half-angle α. Note that a value -1 corresponds to the connection with the lower reservoir and 1 corresponds to the connection with the upper reservoir.*

ΔV *(in* mV*)*	z coordinate (divided by $L/2$) for different α					
	0	2	4	6	8	10
-400	-1	-1	-1	-1.075	-1.075	-1.075
-300	-1	-1	-1	-1.075	-1.075	-1.075
-200	-1.05	-1.05	-1.075	-1.075	-1.075	-1.075
-100	-1.05	-1.05	-1.075	-1.075	-1.075	-1.075
100	1.05	1.05	1.05	1.05	1.05	1.05
200	1.05	1.05	1.05	1.05	1.05	1.05
300	1	1	1	1	1	1
400	1	1	0.925	0.925	0.925	0.925